

Delta-Sigma Modulation for Direct Digital Frequency Synthesis

Dayu Yang, *Member, IEEE*, Fa Foster Dai, *Fellow, IEEE*, Weining Ni, Shi Yin, *Member, IEEE*, and Richard C. Jaeger, *Fellow, IEEE*

Abstract—This paper compares different $\Delta\Sigma$ modulation techniques for direct digital frequency synthesis (DDS). $\Delta\Sigma$ modulators such as MASH, feedforward, feedback, and error feedback have been implemented in both the phase and frequency domains in a CMOS DDS prototype IC fabricated in a 0.35- μm CMOS technology with core area of $1.7 \times 2.1 \text{ mm}^2$ and total current consumption of 75 mA. Measured DDS performance demonstrates that the frequency domain $\Delta\Sigma$ modulation technique achieves better output spectrum purity than the phase domain method. Moreover, a programmable feedforward $\Delta\Sigma$ modulator is proposed to achieve different in-band and out-band noise shaping effects for DDS applications.

Index Terms—CMOS, digital frequency synthesis (DDS), frequency synthesis, noise shaping, signal to noise and distortion ratio (SINAD), spurious free dynamic range (SFDR), $\Delta\Sigma$ modulation.

I. INTRODUCTION

A conventional direct digital synthesizer (DDS) is composed of a numerically controlled oscillator (NCO) and a digital-to-analog converter (DAC) as illustrated in Fig. 1. The NCO further includes a phase accumulator and a ROM lookup table that transforms the accumulated digital phase information to digital amplitude information. Due to the area and power consumption, the phase bits from the accumulator are truncated to reduce the ROM size. The truncated phase error sequence is periodic and causes unwanted spurs in addition to the desired signal in the DDS output spectrum. Nicholas has determined the position and magnitude of these spurs and proposed a method of adding half LSB weight to the phase accumulator to reduce the worst case spur [1]. Other methods of destroying the periodicity of the error sequence such as adding random dither to the phase accumulator was proposed in [2]. $\Delta\Sigma$ modulators have been used in high-performance ADCs, DACs and fractional- N frequency synthesizers and began to appear in the DDS recently. A first-order error feedback type modulator is first adopted in the DDS phase domain to add back the truncated phase information [3]. Second [4] and fourth-order [5] error feedback modulators were introduced in the DDS

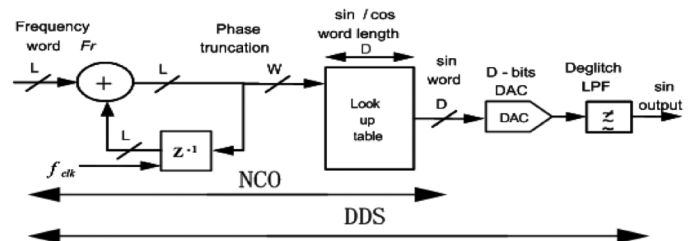


Fig. 1. Conventional direct DDS.

phase domain to reduce spurs in the output spectrum. Song [6] proposed a second order multi loop feedback modulator in the DDS frequency domain. There are other types of modulators that can be used and their noise shaping effects and design tradeoffs have not been thoroughly studied and compared.

In Section II, we will first model the output spurs caused by the phase truncation in an NCO. In order to reduce these phase truncation spurs, $\Delta\Sigma$ modulation is introduced in both phase domain (after the phase accumulator) and frequency domain (before the phase accumulator). Discarded phase or frequency bits due to truncation are fed into a $\Delta\Sigma$ noise shaper and then added back to the remaining phase or frequency word. Because of the high pass noise transfer functions (NTF) of $\Delta\Sigma$ modulators, the spurs as well as the quantization noise can be shifted to a higher frequency band, where they can be removed by the deglitch low-pass filter after the DAC. The output spectrum of a DDS with $\Delta\Sigma$ modulators in both phase and frequency domain can be analyzed using the modulator's white quantization noise model as deduced in Sections II and III.

In Section IV, we discuss the implementation of a CMOS DDS with eight different $\Delta\Sigma$ modulators including MASH, feedforward, feedback and error feedback in both the frequency and phase domains. We compare their noise shaping effects which lead to different in-band spurious free dynamic range (SFDR) and signal to noise and distortion ratio (SINAD). Their operation speeds and stability are also analyzed and compared for different types of modulators.

The noise transfer function of the MASH, feedback and error feedback $\Delta\Sigma$ modulators can be shown to be $(1 - z^{-1})^k$. Although the NTF has sharp in-band noise shaping effect, it has high gain at higher frequencies. As a result, the output of the $\Delta\Sigma$ modulators will dither over a wide range, which causes an increased noise floor at the DDS output. Hence, these $\Delta\Sigma$ modulators require high order filters to remove the magnified high frequency noise. The MASH type $\Delta\Sigma$ modulator can be modified by adding poles to attenuate the high gain at high frequencies. The feedforward $\Delta\Sigma$ modulator is one of the candidates for implementing poles at different locations. The feedforward $\Delta\Sigma$

Manuscript received October 31, 2007; revised February 14, 2008. First published April 28, 2009; current version published May 20, 2009.

D. Yang was with the Department of Electrical and Computer Engineering, Auburn University, Auburn, AL 36839 USA. He is now with Lattice Semiconductor, Bethlehem, PA 18017 USA.

F. F. Dai and R. C. Jaeger are with Department of Electrical and Computer Engineering, Auburn University, Auburn, AL 36839 USA (e-mail: daifa01@eng.auburn.edu; jaeger@eng.auburn.edu).

W. Ni and S. Yin are with the Institute of Semiconductors, Chinese Academy of Sciences, Beijing 100080, China.

Digital Object Identifier 10.1109/TVLSI.2008.2008458

modulator can achieve different NTFs by changing its feedforward coefficients. Thus, it can be used to achieve sharp in-band noise shaping and good out-of-band noise attenuation simultaneously.

The spurious performance of a DDS depends on the input frequency word, the size of the phase accumulator and the number of truncated phase bits. In order to achieve the best spurious performance, speed and power consumption for all the input frequency words, the NTF of the $\Delta\Sigma$ modulator ought to be tunable. We propose a programmable feedforward $\Delta\Sigma$ modulator in Section V that can be adaptively tuned in order to achieve different order, division ratios and different pole locations. The implementation of the programmable $\Delta\Sigma$ modulator with optimized coefficients is discussed in Section VI.

In Section VII, we present results from various different $\Delta\Sigma$ modulators that were implemented in both the frequency and phase domains in a 0.35- μm CMOS DDS IC. The measured DDS output spectra show that the frequency domain $\Delta\Sigma$ modulators have better SFDR and SINAD than their phase domain counterparts. The frequency domain Mash 1-1-1 $\Delta\Sigma$ modulator provides a good noise shaping, fast speed, wide input dynamic range and good stability for DDS applications. The feedforward $\Delta\Sigma$ modulator provides good in-band noise shaping and flat high frequency response.

Conclusions are drawn in Section VIII to summarize the performance of $\Delta\Sigma$ modulators for DDS applications.

II. PHASE DOMAIN $\Delta\Sigma$ MODULATION

In an ideal DDS without phase truncation (i.e., $L = W$) and with infinite amplitude precision, the output sequence of the NCO is given by

$$S(n) = \sin\left(2\pi \frac{Fr}{2^L} n\right) \quad (1)$$

where n represents the number of clock cycles, Fr is the input frequency control word with L bits and W is the length of phase word used to address the ROM lookup table.

In order to reduce the ROM size, one can truncate the phase accumulator output from L bits to W bits. For phase word truncation, we define B to be the number of bits truncated such that $L - W = B$. The output of the NCO becomes

$$S_t(n) = \sin\left(2\pi \frac{2^B}{2^L} \left[\frac{Fr}{2^B} n\right]\right) \quad (2)$$

where the operator $[\]$ represents truncation to the nearest integer value. Equation (2) can alternatively be expressed as

$$S_t(n) = \sin\left(\frac{2\pi}{2^L} (Fr \cdot n - \varepsilon_p(n))\right) \quad (3)$$

where $\varepsilon_p(n)$ represents the phase error sequence due to truncation. Applying trigonometric identities, (3) can be rewritten as

$$S_t(n) = \sin\left(2\pi \frac{Fr \cdot n}{2^L}\right) \cos\left(2\pi \frac{\varepsilon_p(n)}{2^L}\right) - \cos\left(2\pi \frac{Fr \cdot n}{2^L}\right) \sin\left(2\pi \frac{\varepsilon_p(n)}{2^L}\right). \quad (4)$$

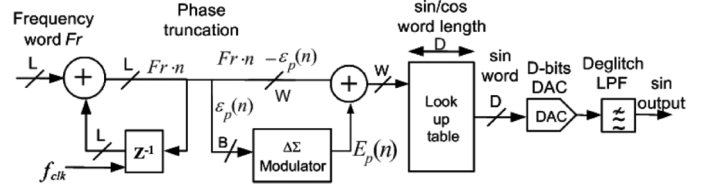


Fig. 2. Phase domain $\Delta\Sigma$ modulation in a DDS.

Assuming phase truncation error $\varepsilon_p(n) \ll 2^L$, we get

$$S_t(n) = \sin\left(2\pi \frac{Fr \cdot n}{2^L}\right) - 2\pi \frac{\varepsilon_p(n)}{2^L} \cdot \cos\left(2\pi \frac{Fr \cdot n}{2^L}\right). \quad (5)$$

Therefore, the output spectrum of the DDS is composed of a sine wave at the desired output frequency corrupted by the cosine harmonics that are amplitude-modulated by the phase error $\varepsilon_p(n)$. The periodic sequence $\varepsilon_p(n)$ can be expressed as Fourier series. Thus, the conventional DDS with phase truncation ends up with spurs at multiple positions in its output spectrum.

In order to reduce spurs due to phase truncation, we apply $\Delta\Sigma$ modulation in the phase domain of a DDS, as shown in Fig. 2. The phase word $Fr \cdot n$ after the accumulator is truncated into $Fr \cdot n - \varepsilon_p(n)$ (W bits) and $\varepsilon_p(n)$ (B bits). Instead of being discarded, the phase error $\varepsilon_p(n)$ is fed into a $\Delta\Sigma$ modulator. The modulator's output $E_p(n)$ is expressed as a single-bit or multi-bit word that is added back to the truncated phase word.

Using a linear model for delta-sigma modulators [7], we get

$$E_p(z) = \varepsilon_p(z) + Q(z)(1 - z^{-1})^k = \varepsilon_p(z) + \text{Noise}(z) \quad (6)$$

where $Q(z)$ is the quantization noise from the quantizer inside the modulator and k is the order of the modulator. We can rewrite (6) as

$$E_p(n) = \varepsilon_p(n) + \text{Noise}(n) \quad (7)$$

where the modulated quantization noise sequence, $\text{Noise}(n)$, is the inverse Z-transform of $Q(z)(1 - z^{-1})^k$, which is high-pass filtered by the modulator.

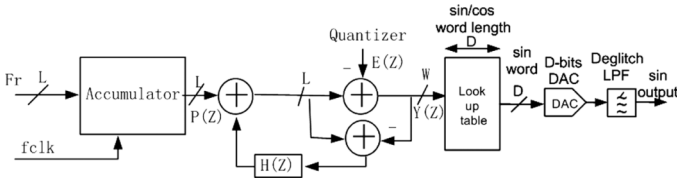
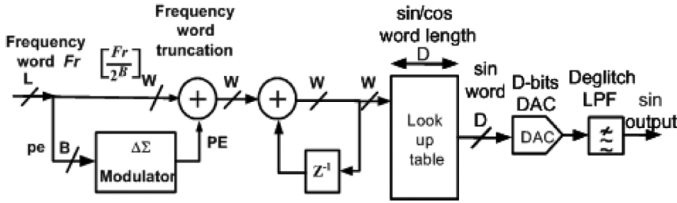
The DDS output is thus given by

$$\begin{aligned} S_t(n) &= \sin\left(\frac{2\pi}{2^L} (Fr \cdot n - \varepsilon_p(n) + E_p(n))\right) \\ &= \sin\left(\frac{2\pi}{2^L} (Fr \cdot n + \text{Noise}(n))\right). \end{aligned} \quad (8)$$

Assuming $\text{Noise}(n) \ll 2^L$, we obtain

$$S_t(n) = \sin\left(2\pi \frac{Fr \cdot n}{2^L}\right) - 2\pi \frac{\text{Noise}(n)}{2^L} \cdot \cos\left(2\pi \frac{Fr \cdot n}{2^L}\right). \quad (9)$$

As a second example, Fig. 3 illustrates the error feedback type of $\Delta\Sigma$ modulator in phase domain. The error feedback $\Delta\Sigma$ modulator was proposed for DDS applications in [4], [5] in first- and fourth-order structures. As shown in Fig. 3, the phase word itself is the input of the modulator. The phase error goes through a filter $H(z)$ and adds back to the phase word. The order and noise transfer function of the $\Delta\Sigma$ modulator are determined


 Fig. 3. Error feedback $\Delta\Sigma$ modulation in a DDS.

 Fig. 4. Proposed DDS with frequency domain $\Delta\Sigma$ modulation.

by feedback transfer function $H(z)$, where the NTF of the $\Delta\Sigma$ modulator is $1 - H(z)$.

The modulator's output can be expressed as $Fr \cdot n + \text{Noise}(n)$, where $\text{Noise}(n)$ is the modulated quantization noise that has been high-pass filtered. Thus, the NCO's output is approaching the desired value expressed in (9). The modulated quantization $\text{Noise}(n)$ replaces the original phase error $\varepsilon_p(n)$. Thus, spurs introduced by the phase truncation are reduced. The modulated quantization noise with high frequency shaping effect shows up in the spectrum. $\Delta\Sigma$ modulators with different noise transfer functions can thus lead to different desired DDS output spectra.

III. FREQUENCY DOMAIN $\Delta\Sigma$ MODULATION

$\Delta\Sigma$ modulation can also be implemented in the frequency domain in a DDS. For frequency word truncation, the frequency word Fr is truncated from L bits to W bits before the phase accumulator, as illustrated in Fig. 4. The discarded frequency bits $B = L - W$, and the output sequence of the DDS ROM becomes

$$\begin{aligned} S(n) &= \sin\left(2\pi \frac{Fr}{2^L} n\right) = \sin\left(2\pi \frac{(Fr/2^B)}{2^W} \cdot n\right) \\ &= \sin\left(2^{1-W} \pi \left(\left[\frac{Fr}{2^B}\right] \cdot n + \left(Fr - \left[\frac{Fr}{2^B}\right] \cdot 2^B\right) \cdot n / (2^B)\right)\right) \\ &= \sin\left(2\pi \left(\left[\frac{Fr}{2^B}\right] n + pe \cdot n\right) / 2^W\right) \end{aligned} \quad (10)$$

where the operator $[]$ represents truncation to an integer, and the frequency error, pe , due to frequency word truncation is given by

$$pe = \left(\left(Fr - \left[\frac{Fr}{2^B}\right] \cdot 2^B\right) / 2^B\right). \quad (11)$$

As shown in (10), the phase accumulator size is reduced to W bits if the input frequency word Fr is truncated to $[Fr/2^B]$.

Frequency word truncation also causes a phase error ($pe \cdot n$) which is periodic in nature and thus leads to spurs at the DDS

output. If the input word $Fr \leq 2^B$, then $[Fr/2^B] = 0$, and there will be no DDS output due to frequency word truncation. However, to avoid losing frequency information, the constant frequency error pe needs to be modulated by a $\Delta\Sigma$ modulator and added back to the accumulator.

In the proposed $\Delta\Sigma$ modulator in the frequency domain shown in Fig. 4, the modulated frequency error pe is added back to the truncated Fr that is represented by $[Fr/2^B]$. Since the input frequency word Fr is a constant, the $\Delta\Sigma$ modulator's input pe is a constant as well, which benefits the modulator's white quantization noise model. The noise shaped frequency error is thus a series of numbers and is given by

$$PE(z) = pe(z) + Q(z)(1 - z^{-1})^k = pe(z) + \text{Noise}(z) \quad (12)$$

where $Q(z)$ is the quantization noise introduced by the frequency word truncation.

With frequency domain $\Delta\Sigma$ modulation, the DDS ROM output is given by

$$\begin{aligned} S_t(n) &= \sin 2\pi \left(\left[\frac{Fr}{2^B}\right] n + PE(n) \cdot n\right) / 2^W \\ &= \sin 2\pi \left(\left[\frac{Fr}{2^B}\right] n + pe \cdot n + \text{Noise}(n) \cdot n\right) / 2^W \\ &\approx \sin\left(2\pi \frac{Fr \cdot n}{2^L}\right) - \cos\left(2\pi \frac{Fr \cdot n}{2^L}\right) \\ &\quad \cdot \left(2\pi \frac{\text{Noise}(n) \cdot n}{2^W}\right). \end{aligned} \quad (13)$$

Thus, the DDS output spectrum is composed of a sine wave at the desired output frequency and a cosine wave that is modulated by the quantization noise that is shaped by the $\Delta\Sigma$ modulator. Based on the previous linear model for $\Delta\Sigma$ modulation, the periodic phase error due to frequency word truncation is reduced in the signal band and is shifted to the higher frequency band, where it can be easily removed by the low-pass filter (LPF) after the DAC.

IV. COMPARISON OF THE PERFORMANCE OF DIFFERENT $\Delta\Sigma$ MODULATORS

Although $\Delta\Sigma$ modulators in both the phase and frequency domains can move the spurs and quantization noise to a higher frequencies, their noise shaping behaviors are not same. To compare different $\Delta\Sigma$ modulators, we consider factors such as the modulator topology, the order of the modulator, the modulator input, the in-band spurious tones, the number of quantizer bits, and the modulator speed and area. We first implemented an NCO with several types of $\Delta\Sigma$ modulators in both frequency and phase domains using an FPGA as shown in Fig. 5. The NCO output is captured into a computer for analysis. First we analyze the output characteristics such as the spurious-free-dynamic-range (SFDR), defined as the ratio between the fundamental signal and the largest spur and the signal-to-noise-and-distortion ratio (SINAD) defined as

$$\text{SINAD} = 20 \cdot \log\left(\frac{\text{Signal}}{\sum(\text{Noise} + \text{Harmonics})}\right). \quad (14)$$

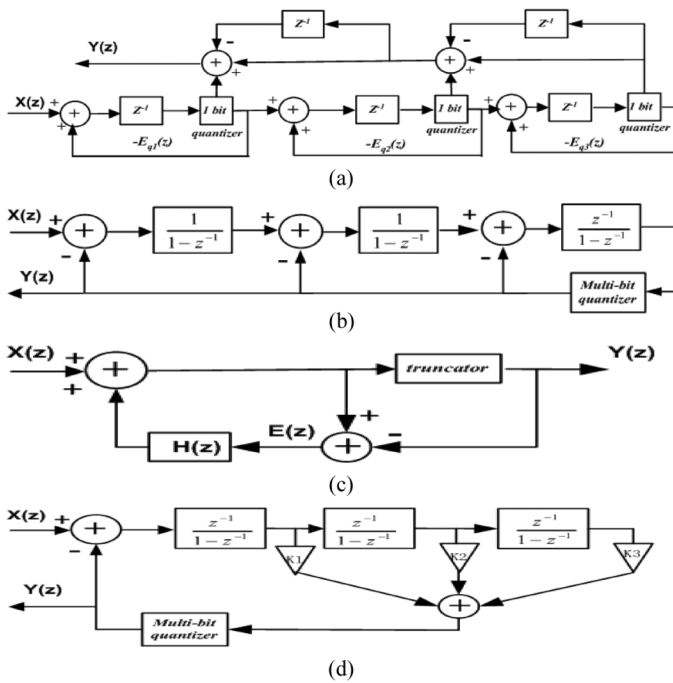


Fig. 5. Four types of $\Delta\Sigma$ modulators implemented in the DDS. (a) MASH 1-1-1. (b) Third-order feedback. (c) Error feedback. (d) Third-order feedforward.

The oversampling ratio (OSR) of the $\Delta\Sigma$ modulator is chosen as 64 and the band of interest is from dc to $1/64$ of the clock frequency. The measured in-band SINAD and SFDR of the NCO output with different $\Delta\Sigma$ modulators are given in Fig. 6. The third-order Feedforward modulator has coefficients of $k_1 = 2$, $k_2 = 1.5$, $k_3 = 0.5$ while the new third-order Feedforward modulator has different coefficients of $k_1 = 2.2$, $k_2 = 1.92$, $k_3 = 0.72$. The measurements show that the DDS with direct phase truncation (without $\Delta\Sigma$ modulation) has the lowest SFDR and SINAD. With $\Delta\Sigma$ modulation, the in-band SFDR and SINAD have an improvement of around 10 dB. Frequency domain $\Delta\Sigma$ modulation has an additional 10 dB higher SFDR and SINAD than the phase domain counterpart. Although using a high-order $\Delta\Sigma$ modulator results in a sharper noise shaping slope, its output has wider bit patterns to degrade the SFDR and SINAD shown in Fig. 6.

Since the modulated quantization noise dominates the DDS output spectrum, its noise transfer function $H_e(z)$ greatly affects the DDS spectrum purity. We implemented four types of $\Delta\Sigma$ modulators, i.e., MASH, feedforward, feedback and error feedback as shown in Fig. 5. Although MASH, feedback and error feedback type $\Delta\Sigma$ modulators have the same noise transfer function of $H_e(z) = (1 - z^{-1})^k$, they are quite different in implementation. MASH and error feedback modulators both have a single-bit quantizer, while the feedback modulator has a multi-bit quantizer. A feedforward type modulator's NTF has more variety by varying the feedforward coefficients k_1, k_2, k_3 , and one modulator with coefficients of $k_1 = 2.2$, $k_2 = 1.92$, $k_3 = 0.72$ was first implemented in [10] and here we name it Feedforward2 for later comparison.

Fig. 7 compares the noise transfer function of a prior art MASH, a Feedforward1 modulator [8], and the implemented Feedforward2 modulator [10]. It is clear that MASH has much

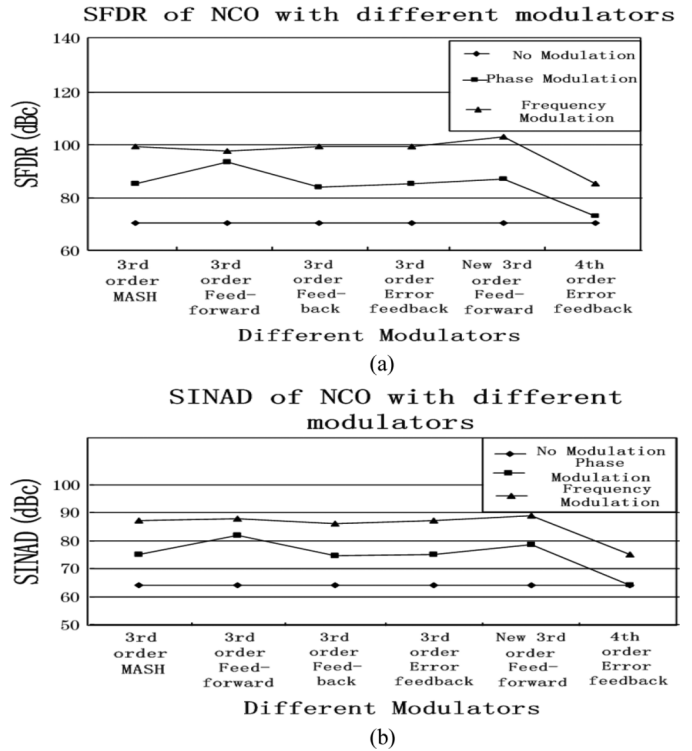


Fig. 6. Measured in-band SINAD (a) and SFDR (b) at the NCO output with various $\Delta\Sigma$ modulators in frequency and phase domains.

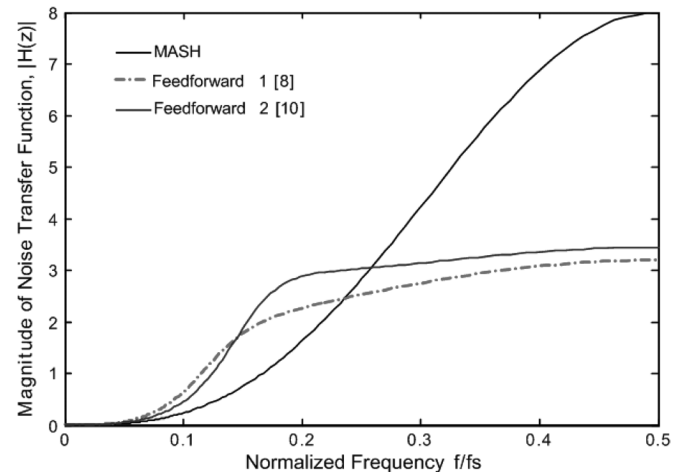


Fig. 7. Simulated noise transfer function of MASH and feedforward $\Delta\Sigma$ modulators.

sharper noise shaping effect at in-band, yet it has high out-of-band noise that requires a high-order LPF for noise rejection. The Feedforward2 modulator has lower in-band noise compared with the existing Feedforward1 modulator and has flat out-of-band noise compared with the MASH type.

Fig. 8 gives the measured NCO output spectrum for two types of $\Delta\Sigma$ modulators. The measured spectra of the two $\Delta\Sigma$ modulators are almost identical with the modulated noise. The multi-bit quantizer allows the feedback signal to match the input signal more accurately and results in a more randomly distributed output pattern, which better fits the linear model for $\Delta\Sigma$ modulators.

The MASH type modulator is famous for its stability. It is also good for high speed implementation for it has only one

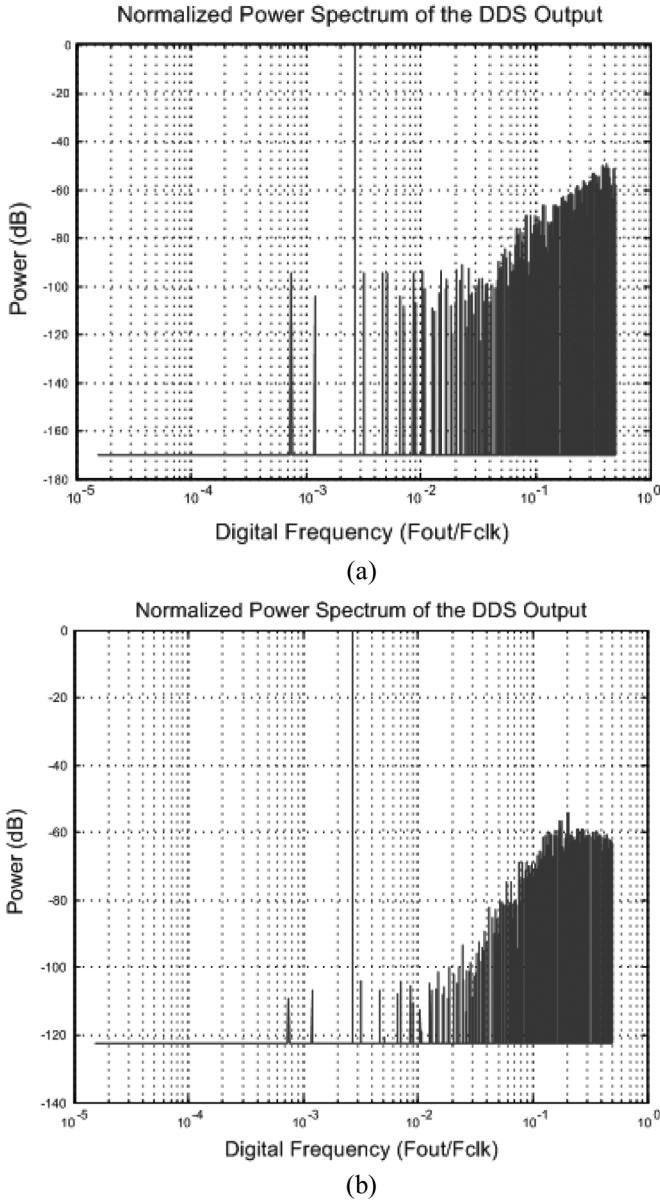


Fig. 8. Comparison of measured NCO output spectra with $\Delta\Sigma$ modulators. (a) NCO output spectrum with third MASH type delta- $\Delta\Sigma$ modulator in frequency domain (1-bit quantizer). (b) NCO output spectrum with frequency domain third-order Feedforward2 $\Delta\Sigma$ modulator (multi-bit quantizer).

path from its input to the output instead of a feedback loop, so the retiming method can be applied to shorten the critical path between registers. As shown in Fig. 9, several registers are pushed from the input to the output until the critical path contains only one adder between two adjacent registers. So the maximum speed is limited only by one n -bit adder. The drawback of the MASH modulator lies on its fixed number of output bits and its infinite gain at high frequency. Error feedback has the same noise transfer function as that of the MASH, yet it operates at lower speed due to the multiple adders in the feedback path. However, an error feedback modulator can flexibly choose the number of output bits. The feedback modulator has the same noise transfer function as MASH and also has an advantage of a multi-bit quantizer, but it has limited input stability range. The

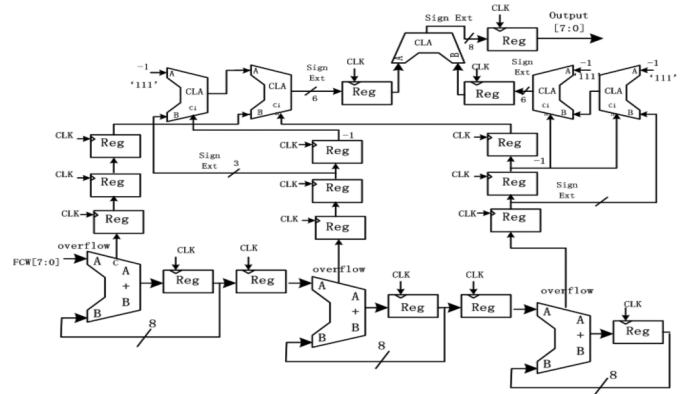


Fig. 9. Retiming registers in MASH modulator.

proposed Feedforward2 $\Delta\Sigma$ modulator has good in-band noise shaping and flat out-band gain. However, its implementation requires more hardware, and its speed is lower.

V. PROPOSED PROGRAMMABLE FEEDFORWARD $\Delta\Sigma$ MODULATOR

The feedforward $\Delta\Sigma$ modulator has the advantage of flexibly placing its poles inside the unit circle in the z -domain by changing its feed-forward coefficients. In hardware implementation, those coefficients are chosen to be times of 2 for easy implementation using shift operations. This also leads to faster speed compared with implementations using multiplications. The design goal of a feedforward modulator is to achieve sharper noise shaping in-band, as close as to that of MASH. Meanwhile, it needs to constrain the out-band gain. The widespread output values lead to a wide spread of the ROM addressing around the desired value, which degrades the DDS output spectrum purity.

We therefore propose a programmable feedforward $\Delta\Sigma$ modulator for frequency synthesis, as depicted in Fig. 10. Input $X(z)$ is extended to L bits before it goes to the modulator. The modulator's output $Y(z)$ is the truncated signal from its quantizer. The quantization noise transfer function of the proposed $\Delta\Sigma$ modulator can be found to be

$$H_E(z) = \frac{(z-1)^n}{(z-1)^n + \sum_{i=1}^n K_i(z-1)^{n-i}} \quad (15)$$

where n is the number of accumulators in the feedforward loop and represents the order of the modulator. Each accumulator output is multiplied by a feedforward coefficient K_i before it is fed to an adder. The poles of the NTF can be adjusted by choosing different tap coefficients. Thus, the noise shaping effect of the modulator can be adapted based on system requirements. The order of the accumulator is reconfigurable by setting some feedforward coefficients K_i to zero. For instance, with four accumulators, $n = 4$, we can get a third-order modulator by setting $K_4 = 0$ and a second-order modulator by setting $K_3 = K_4 = 0$.

Different coefficients lead to different noise shaping effect by NTFs, and modulator has programmable coefficients that allow

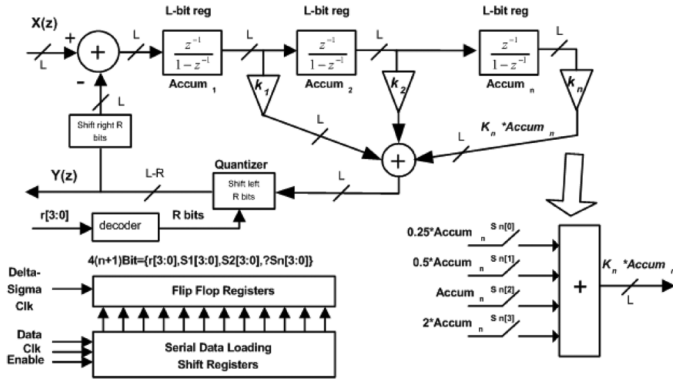


Fig. 10. Proposed programmable feedforward $\Delta\Sigma$ modulator for frequency synthesis.

TABLE I
SHIFTING OPERATIONS

$5 * \text{Accum}_n = \{\text{Accum}_n[L-1], \text{Accum}_n[L-1], \text{Accum}_n[L-1:2]\}$
$0.5 * \text{Accum}_n = \{\text{Accum}_n[L-1], \text{Accum}_n[L-1:1]\}$
$1 * \text{Accum}_n = \text{Accum}_n$
$2 * \text{Accum}_n = \{\text{Accum}_n[L-1], \text{Accum}_n[L-3:0], 1'b0\}$

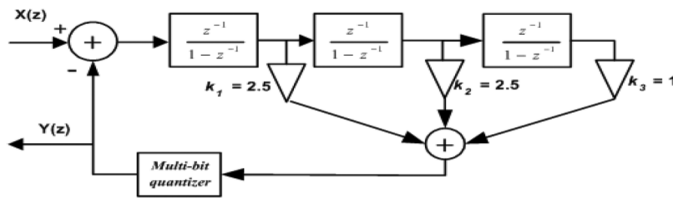
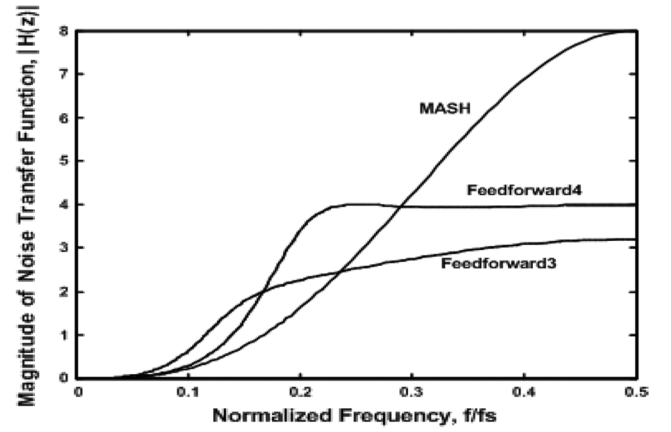


Fig. 11. Block diagram illustrating the proposed third-order Feedforward4 $\Delta\Sigma$ modulator.

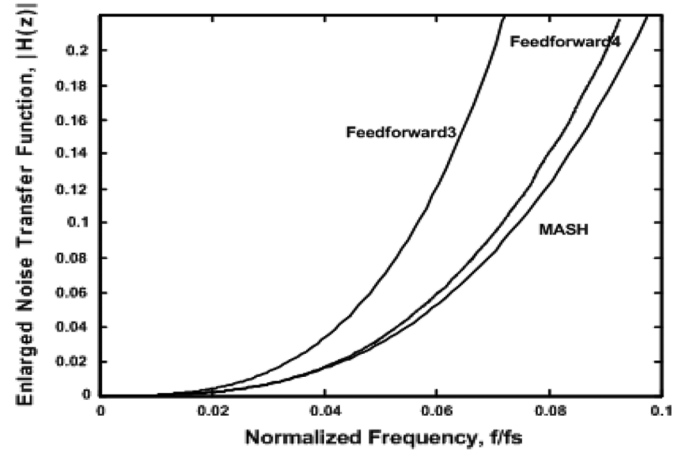
programming of the NTF. Although a coefficient can be modulated to a digital word by using a digital multiplier, its implementation has area and speed limits. The coefficients in this $\Delta\Sigma$ modulator are implemented using only shifting and addition operations. As shown in Fig. 10, in order to multiply the n th accumulator's output Accum_n with K_n , Accum_n is shifted to $0.25 * \text{Accum}_n$, $0.5 * \text{Accum}_n$, Accum_n and $2 * \text{Accum}_n$ before being fed into an adder. In this way, a coefficient K_n that ranges from 0 to 3.75 with an increment of 0.25 can be realized by loading the desired control signals $\text{Sn}[3]$, $\text{Sn}[2]$, $\text{Sn}[1]$, $\text{Sn}[0]$ from the input serial registers. If $K_n = 1.75$, $\text{Sn}[3]$, $\text{Sn}[2]$, $\text{Sn}[1]$, $\text{Sn}[0]$ are set to "0 1 1 1". If $K_n = 0$, $\text{Sn}[3]$, $\text{Sn}[2]$, $\text{Sn}[1]$, $\text{Sn}[0]$ are set to "0 0 0 0".

Since all data are binary weighted, for an accumulator with L -bit length ($\text{Accum}_n[L-1:0]$), the shifting operations are shown in Table I, where Verilog notation of concatenation " $\{ \}$ " was used. Note that the most important four bits of Accum_n are the sign extension bits and only mark the sign of the value in the accumulator. This is to make sure the sign bit information is not lost if the accumulator is right or left shifted 1~2 bits.

The division ratio of the $\Delta\Sigma$ modulator is also reconfigurable by setting the truncated R bits of its quantizer. The quantizer truncates the least significant R bits and outputs Y with $L - R$ bits. The feedback is left shifted R bits with its least significant R bits being zeros. Thus we can get variable division ratios in the $\Delta\Sigma$ modulator. The output of the $\Delta\Sigma$ modulator Y represents a



(a)



(b)

Fig. 12. Simulated NTF of MASH, Feedforward3 and Feedforward4 $\Delta\Sigma$ modulators. (a) Nyquist band NTF. (b) In-band NTF.

fractional value $X/2^R$, ($X < 2^R$). The ratio control bits R can be loaded through a serial data loading shift register as shown in Fig. 10.

VI. IMPLEMENTATION OF THE PROPOSED $\Delta\Sigma$ MODULATOR FOR DDS APPLICATIONS

As an example of the proposed programmable feedforward $\Delta\Sigma$ modulator, we implemented a third order feedforward $\Delta\Sigma$ modulator that has the same NTF given in [8], where three output bits were used. The peak of the quantization noise was flattened by introducing an extra pole into the digital modulator. This approach helped meet phase noise specifications at high frequency offsets while still using a high-order modulator. The disadvantage of this architecture is increased in-band noise compared to MASH $\Delta\Sigma$ modulator.

The noise transfer functions of the Feedforward3 $\Delta\Sigma$ modulator presented in [8] is given by

$$\begin{aligned} H_{E3}(z) &= \frac{(z-1)^3}{(z-1)^3 + 2(z-1)^2 + 1.5(z-1) + 0.5} \\ &= \frac{(1-z^{-1})^3}{1-z^{-1} + 0.5z^{-2}}. \end{aligned} \quad (16)$$

It can be seen that the $\Delta\Sigma$ modulator adds two low-Q Butterworth poles in addition to the three zeros at $z = 1$ found in the

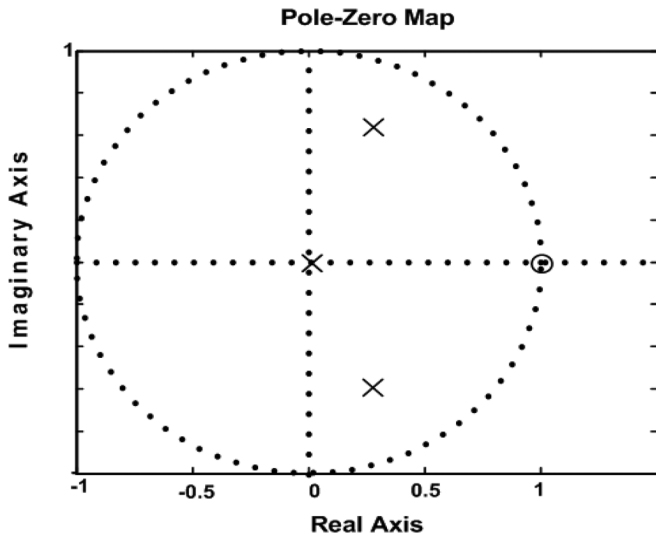


Fig. 13. NTF pole-zero map of the Feedforward4 $\Delta\Sigma$ modulator.

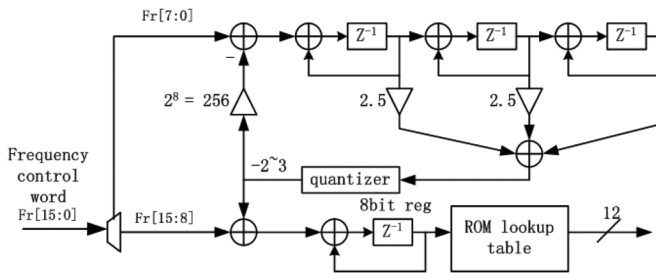


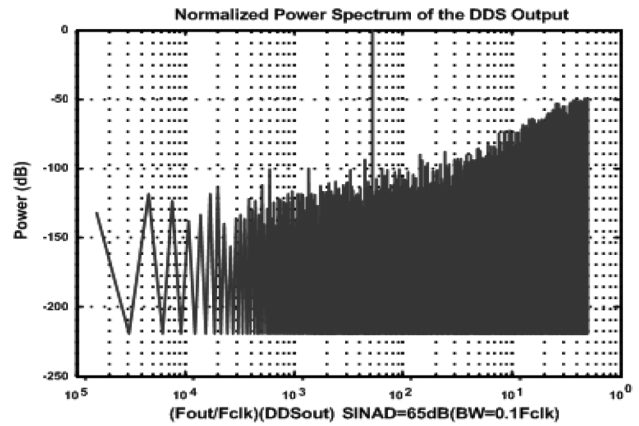
Fig. 14. NCO with Feedforward4 $\Delta\Sigma$ modulator.

standard MASH 1-1-1 structure. All the poles are located inside the unit circle. Thus, the modulator is stable.

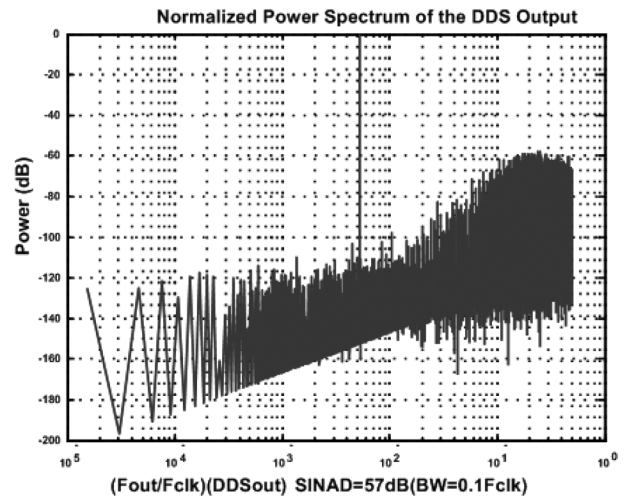
The previous Feedforward3 $\Delta\Sigma$ modulator has the drawback of poor in-band noise shaping. We use the proposed programmable feedforward $\Delta\Sigma$ modulator architecture to implement a new third-order Feedforward4 $\Delta\Sigma$ modulator with new set of coefficients $k_1 = 2.5, k_2 = 2.5, k_3 = 1$, as illustrated in Fig. 11. The noise transfer functions of the Feedforward4 modulator presented in Fig. 11 is given by

$$H_{EA}(z) = \frac{(z - 1)^3}{(z - 1)^3 + [2.5(z - 1)^2 + 2.5(z - 1) + 1]} = \frac{(1 - z^{-1})^3}{1 - 0.5z^{-1} + 0.5z^{-2}} \quad (17)$$

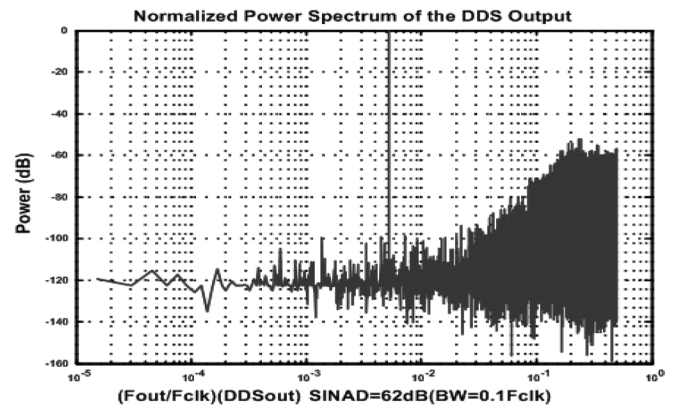
Fig. 12 compares the noise transfer function of MASH, Feedforward3 [8], and the proposed Feedforward4 $\Delta\Sigma$ modulators. It is clear that the MASH modulator has sharper in-band noise shaping, but it has high out-of-band noise that requires a high-order LPF for noise rejection. The Feedforward4 modulator has lower in-band noise compared with the Feedforward3 modulator and has flat out-of-band noise compared with the MASH type. Thus, the in-band SINAD of the DDS output is increased compared to that of the Feedforward3 type, it has less out-of-band noise compared with the MASH type. The poles and zeros of the proposed modulator are shown in Fig. 13, indicating modulator stability.



(a)



(b)



(c)

Fig. 15. Comparison of Measured NCO output spectrum with different noise shaping effects. (a) NCO output spectrum with frequency domain third-order MASH type $\Delta\Sigma$ modulator. (b) NCO output spectrum with frequency domain third-order Feedforward1 [8] $\Delta\Sigma$ modulator. (c) NCO output spectrum with the proposed frequency domain third-order Feedforward2 $\Delta\Sigma$ modulator.

Fig. 14 illustrates an NCO structure with the proposed modulator. The three coefficients of the modulator are chosen as $k_1 = 2.5, k_2 = 2.5, k_3 = 1$. The 16-bit frequency word Fr is truncated to the most significant 8 bits $Fr[15:8]$. The least significant 8 bits $Fr[7:0]$ are fed into the proposed modulator. The modulator's division parameter R is programmed as 8 since the

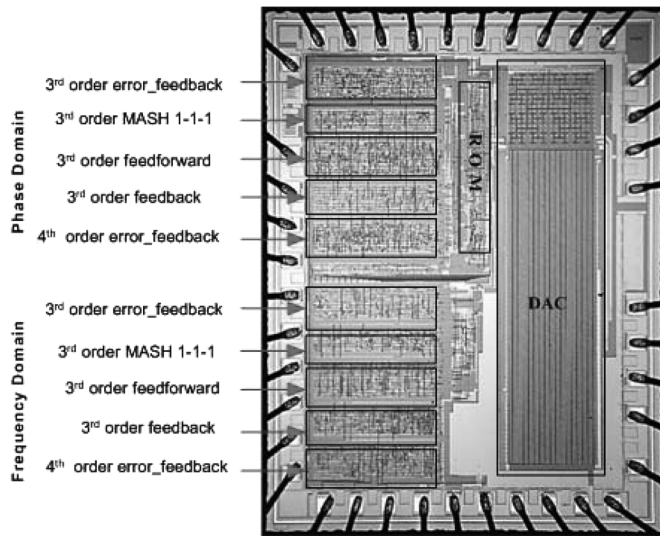


Fig. 16. Die photo of the CMOS DDS prototype chip with various $\Delta\Sigma$ modulators in frequency and phase domain.

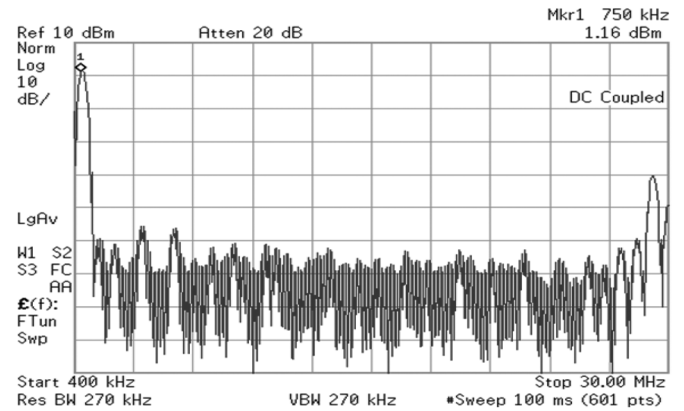
frequency truncation bit is 8. Its output ranges from -2 to 3 and is added back to the most significant 8 bits $Fr[15:8]$. The modulated frequency control word goes to an 8-bit phase accumulator. The phase information from the accumulator addresses the ROM, and the ROM generates a 12-bit digital sine wave at the NCO output.

Fig. 15 gives the simulated NCO output spectra and the in-band SINAD comparisons for three types of $\Delta\Sigma$ modulators. The proposed Feedforward2 type modulator achieves more than 5 dB improvement in SINAD for in-band (dc to 0.1 fs) than the Feedforward1 type proposed in [8]. The proposed Feedforward2 $\Delta\Sigma$ modulator also presents a flat out-band noise compared to the MASH type structure and relaxes the filter design.

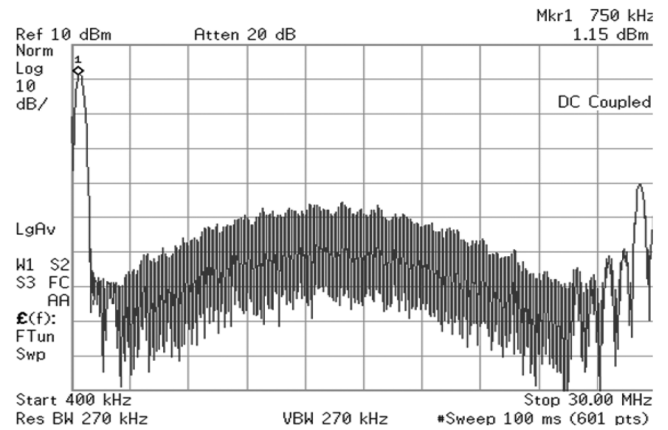
The above NCO discussion can be directly applied to a DDS with an ideal DAC and LPF. But a finite resolution DAC also affects the SFDR and SINAD of the DDS output. Normally, the DAC bits are set to be the limiting factor of DDS performance, and hence the number of phase bits W should be equal or bigger than the number of DAC bits D . However, with $\Delta\Sigma$ modulator added to the DDS, the in-band noise can be further modulated and pushed to higher frequency and the W can be set less than D to save area and power.

VII. IMPLEMENTATION OF THE CMOS DDS WITH DIFFERENT $\Delta\Sigma$ MODULATORS OF THE PROPOSED $\Delta\Sigma$ MODULATOR FOR DDS APPLICATIONS

To compare DDS performance with different $\Delta\Sigma$ modulation, we designed a DDS chip that contains different $\Delta\Sigma$ modulators including MASH1-1-1, third-order feedforward, feedback and error feedback $\Delta\Sigma$ modulators as shown in Fig. 5 in both frequency and phase domains. Different $\Delta\Sigma$ modulators can be selected individually while other $\Delta\Sigma$ modulators are turned off. The DDS prototype with both frequency domain and phase domain $\Delta\Sigma$ modulators was implemented in a $0.35\text{-}\mu\text{m}$ CMOS technology with two poly and four metal layers. A 16-bit



(a)



(b)

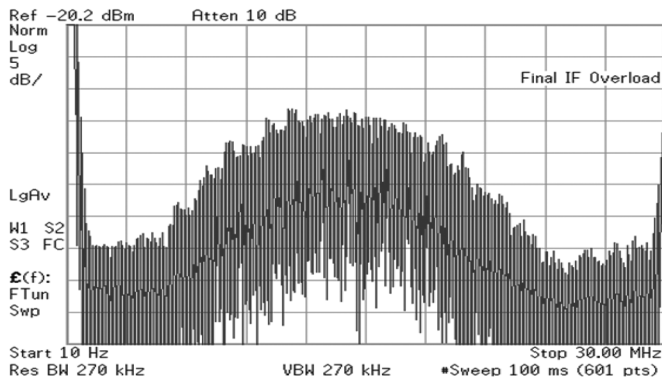
Fig. 17. Comparison of the measured output spectra for (a) conventional DDS without $\Delta\Sigma$ modulation and (b) proposed DDS with frequency domain third-order MASH type $\Delta\Sigma$ modulation, $f_o = 750$ KHz, $f_{clk} = 30$ MHz. (a) Without $\Delta\Sigma$ modulator; (b) with frequency domain third-order MASH $\Delta\Sigma$ modulator.

accumulator is used, and 8 phase bits are used for addressing the look-up ROM. A 12-bit current steering DAC is integrated to convert the ROM output to an analog signal. For 12-bit amplitude resolution in a conventional DDS without a $\Delta\Sigma$ modulator, at least 12 phase bits should be used, which requires a look-up ROM with 212×12 bits. The use of a $\Delta\Sigma$ noise shaper effectively reduces the required number of phase bits. Thus, we use only 8 phase bits to address the ROM, which reduces the ROM size by a factor of 24 or 16 times compared to that of a conventional DDS without a $\Delta\Sigma$ modulator [5].

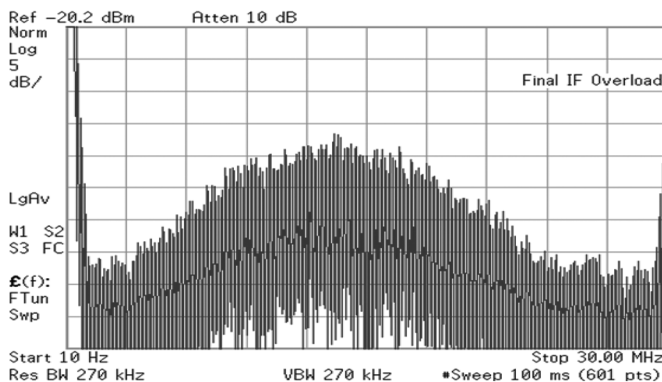
The die photo of the fabricated CMOS $\Delta\Sigma$ DDS prototype chip is shown in Fig. 16. The total die area is 2×2.5 mm², in which the DDS active core area is 1.7×2.1 mm² including the DAC, and the rest of the die area is used for pads and ESD diodes. The 16-bit phase accumulator and ten $\Delta\Sigma$ modulators occupy 0.7×2.1 mm² die area. The 28×12 -bit ROM occupies only 0.1×0.8 mm², which would be 16 times larger without the $\Delta\Sigma$ noise shaper. In a conventional DDS, the ROM normally takes the majority of the die area, whereas the ROM takes only a small portion of the total area in this DDS implementation, which clearly demonstrates the advantage of using $\Delta\Sigma$ noise shaping in DDS designs.

TABLE II
PERFORMANCE COMPARISON OF $\Delta\Sigma$ MODULATORS IN FREQUENCY AND PHASE DOMAINS FOR DDS APPLICATIONS

Frequency domain	High freq. noise	Modulator output range (bits)	In-band SFDR of NCO (dBc)	In-band SINAD of NCO (dBc)	Stability	Area (mm ²)	Speed (Mhz)
3 rd order MASH 111	poor	-3~4	99	87	stable	0.112	180
3 rd order Feedback	fair	-3~4	99	86	fair	0.126	140
3 rd order Feedforward	good	-2~3	103	89	stable	0.161	150
3 rd order Error Feedback	poor	-3~4	99	87	good	0.147	140
4 th order Error Feedback	poor	-7~8	85	75	good	0.148	160
Phase domain							
3 rd order MASH 111	poor	-3~4	85	75	stable	0.112	180
3 rd order Feedback	fair	-3~4	84	74	fair	0.126	140
3 rd order Feedforward	good	-2~3	87	78	stable	0.161	150
3 rd order Error Feedback	fair	-3~4	85	75	good	0.147	140
4 th order Error Feedback	poor	-7~8	73	64	good	0.148	160



(a)



(b)

Fig. 18. Measured DDS output spectra with fourth-order error feedback type $\Delta\Sigma$ modulations. (a) Phase domain; (b) frequency domain.

The measured DDS output spectra with and without $\Delta\Sigma$ modulators are shown in Fig. 17. It is clear that the in-band spurs without a $\Delta\Sigma$ modulator [see Fig. 17(a)] are reduced by using a third-order MASH type $\Delta\Sigma$ modulator [see Fig. 17(b)]. Fig. 18 demonstrates the DDS output spectra with a fourth-order $\Delta\Sigma$ modulator in the phase domain [see Fig. 18(a)] and in the frequency domain [see Fig. 18(b)]. The frequency domain modulation achieves better in-band SINAD and SFDR. Table II compares the performance of the other different types and different orders of $\Delta\Sigma$ modulators in the phase or frequency domain. The in-band SFDR and SINAD are measured from the NCO output. On the other hand, the number of output bit patterns which relates to the out-band noise needs to be

restrained, for it can lead to poor in-band SINAD and SRDR. Fourth-order $\Delta\Sigma$ modulation is thus not as good as a third order modulator. The proposed new third-order feedforward type $\Delta\Sigma$ can achieve both good in-band noise shaping and low out-band noise.

In Table II, we can see that the DDS with frequency domain $\Delta\Sigma$ modulation achieves better SFDR and SINAD than its phase domain counterpart. Every $\Delta\Sigma$ modulator except multi-loop feedback is stable and has an input range from 1~255. The MASH 1-1-1 $\Delta\Sigma$ modulator in the frequency domain provides good noise shaping for DDS application with best speed and area consumption. Feedforward $\Delta\Sigma$ modulator with programmable coefficients can provide both good in-band noise shaping and flat high frequency performance, and constrains the modulator’s output to be within $-2 \sim 3$. It yields the best in-band SFDR and SINAD, but it takes additional area.

VIII. CONCLUSION

Direct digital synthesis with $\Delta\Sigma$ modulation consumes much less hardware and power and can synthesize sine waveforms with high in-band SFDR and SINAD. We have explained the spur reduction effects of $\Delta\Sigma$ modulation in both the frequency and phase domains and conclude that the modulated quantization noise takes the place of the spurs in DDS output. Various $\Delta\Sigma$ modulators with different noise shaping effects in both the frequency and phase domains were implemented in a 0.35 μm CMOS DDS prototype chip to compare their performance. The measured data demonstrates frequency domain modulation is better in in-band spur reduction than phase domain modulation. In addition, a programmable $\Delta\Sigma$ feedforward modulator architecture is proposed for DDS applications. The order, division ratio and the feedforward coefficients of the $\Delta\Sigma$ feedforward modulator can be programmed to achieve different noise transfer functions. We have also proposed a third order feedforward type $\Delta\Sigma$ modulator with coefficients of $k_1 = 2.5$, $k_2 = 2.5$, and $k_3 = 1$. The proposed $\Delta\Sigma$ modulator shows sharp in-band noise shaping with attenuated out-band gain, and it achieves a 5 dB SINAD improvement in DDS output performance compared to the use of the existing $\Delta\Sigma$ modulator [8].

REFERENCES

[1] H. T. Nicholas, III and H. Samuelli, “An analysis of the output spectrum of direct digital frequency synthesizers in the presence of phase-accumulator truncation,” in *Proc. 41st Ann. Freq. Control Symp.*, 1987, pp. 495–502.

- [2] J. Vankka, "Spur reduction techniques in sine output direct digital synthesis," in *Proc. IEEE Int. Freq. Control Symp.*, 1996, pp. 951–959.
- [3] P. O'Leary and F. Maloberti, "A direct-digital synthesizer with improved spectral performance," *IEEE Trans. Commun.*, vol. 39, no. 7, pp. 1046–1048, Jul. 1991.
- [4] J. Vankka, "A direct digital synthesizer with a tunable error feedback structure," *IEEE Trans. Commun.*, vol. 45, no. 4, pp. 416–420, Apr. 1997.
- [5] F. F. Dai, W. Ni, S. Yin, and R. C. Jaeger, "A direct digital frequency synthesizer with single-stage $\Delta\Sigma$ interpolator and current-steering DAC," *IEEE J. Solid State Circuits*, vol. 41, no. 4, pp. 839–850, April 2006.
- [6] Y. Song and B. Kim, "A 250 MHz direct digital frequency synthesizer with $\Delta\Sigma$ noise shaping," in *Proc. IEEE Int. Solid-State Circuits Conf. (ISSCC)*, 2003, pp. 472–473.
- [7] S. R. Norsworthy, R. Schreier, and G. C. Temes, *Delta-Sigma Data Converters, Theory, Design and Simulation*. Piscataway, NJ: IEEE Press, 1997.
- [8] W. Rhee, B.-S. Song, and A. Ali, "A 1.1-GHz CMOS fractional-N frequency synthesizer with a 3-b third-order $\Delta\Sigma$ modulator," *IEEE J. Solid State Circuits*, vol. 35, no. 10, pp. 1453–1460, Oct. 2000.
- [9] P. O'Leary and F. Maloberti, "A direct-digital synthesizer with improved spectral performance," *IEEE Trans. Commun.*, vol. 39, no. 7, pp. 1046–1048, Jul. 1991.
- [10] D. Yang, W. Ni, F. F. Dai, S. Yin, and R. C. Jaeger, "Delta-sigma modulation in direct digital frequency synthesis," in *Proc. IEEE Custom Integr. Circuits Conf.*, San Jose, CA, Sep. 2006, pp. 523–526.



Dayu Yang (S'04–M'07) received the B.S. and M.S. degrees in electrical engineering from Shanghai Jiao Tong University, Shanghai, China, in 1999 and 2002, respectively, and the Ph.D. degree in electrical and computer engineering from Auburn University, Auburn, AL, in 2006.

From 2006, he has been with Lattice Semiconductor, Bethlehem, PA, where he is involved with clocking, routing and SerDes circuits design for FPGA. From 2002 to 2003, he was a Design Engineer with Pericom Technology, Shanghai, China,

where he was involved with the design of ADC and oscillators for remote control chip. His research interests include delta-sigma modulation, direct and PLL frequency synthesis and SerDes circuit design.

Dr. Yang is a member of Sigma Xi.



Fa Foster Dai (M'92–SM'00–F'09) received the Ph.D. degree in electrical and computer engineering from Auburn University, Auburn, AL, in 1997, and the Ph.D. degree in electrical engineering from The Pennsylvania State University, Philadelphia, PA, in 1998.

From 1997 to 2000, he was with Hughes Network Systems of Hughes Electronics, Germantown, MD, where he was a Member of Technical Staff in very large scale integration (VLSI), designing analog and digital ICs for wireless and satellite communications.

From 2000 to 2001, he was with YAFO Networks, Hanover, MD, where he was a Technical Manager and a Principal Engineer in VLSI designs, leading high-speed SiGe IC designs for fiber communications. From 2001 to 2002, he was with Cognio Inc., Gaithersburg, MD, designing radio frequency (RF) ICs for integrated multi-band MIMO wireless transceivers. From 2002 to 2004, he was an RFIC consultant for Cognio Inc. In August 2002, he joined Auburn University, Auburn, AL, where he is currently a Professor in electrical and computer engineering. His research interests include VLSI circuits for analog and mixed-signal applications, RFIC designs for wireless and broadband networks, ultra-high frequency synthesis and mixed signal built-in self-test (BIST). He coauthored the book *Integrated Circuit Design for High-Speed Frequency Synthesis* (Artech, 2006).

Dr. Dai has served as Guest Editors for IEEE TRANSACTIONS ON INDUSTRIAL ELECTRONICS in 2001, 2008 and 2009. He served on the technical program committees of the IEEE Symposium on VLSI Circuits from 2005 to 2008. He was the Co-Chair of the wireless workshop on Multi-Standard Wireless Transceiver RFIC Designs at 2007 IEEE Symposium on VLSI Circuits. He currently

serves on the technical program committees of the IEEE Custom Integrated Circuits Conference (CICC), the IEEE Bipolar / BiCMOS Circuits and Technology Meeting (BCTM) and the IEEE Topical Meeting on Silicon Monolithic Integrated Circuits in RF Systems (SiRF). He was elected IEEE Fellow in 2009 "for contributions to high-speed frequency synthesis and radio frequency integrated circuits". He received the Research Award for Excellence from the College of Engineering of Auburn University in 2009."



Weining Ni received the B.S. and M.S. degrees in electrical engineering and control engineering from the China Petroleum University, Shandong, China, in 2000 and 2003, respectively, and the Ph.D. degree in microelectronic at Institute of Semiconductors, Chinese Academy of Sciences (CAS), Beijing, China, in 2006.

His research interests include high speed analog and mixed-signal VLSI circuit design.



Shi Yin (M'05) received the M.Sc. degree in electrical engineering and the Ph.D. degree from the Chinese Academy of Science, Beijing, China, in 1981 and 1986, respectively.

Currently, he is a Professor and a Ph.D. supervisor with the Institute of Semiconductors, Chinese Academy of Sciences. His research interests include the area of mixed-signal circuit designs.



Richard C. Jaeger (F'86) was born in New York on September 2, 1944. He received the B.S. and M.E. degrees in electrical engineering and the Ph.D. degree from the University of Florida, Gainesville, in 1966, 1966, and 1969, respectively.

From 1969 to 1979, he was with the IBM Corporation working on precision analog design, I2L, microprocessor architecture, and low temperature MOS device and circuit behavior. He holds three patents and received two Invention Achievement Awards from the IBM Corporation. In 1979, he

joined Auburn University where he is Distinguished University Professor in electrical and computer engineering and served as Director of the Alabama Microelectronics Science and Technology Center from 1984 through 2000. During 2001–2004, he led implementation of Auburn University's new Bachelor of Wireless Engineering degree program, an interdisciplinary effort of the ECE and CSSE departments. He has published over 200 technical papers and articles, and authored or coauthored *Introduction to Microelectronic Fabrication (2E)*, *Microelectronic Circuit Design (2E)*, and *Computerized Circuit Design Using SPICE Programs*.

Dr. Jaeger was a recipient of the IEEE Education Society Jacob Millman/McGraw-Hill Award for outstanding textbook development in 1998 and received the IEEE Undergraduate Teaching Award in 2004. He was a member of the IEEE Solid-State Circuits Council from 1984–1991, serving the last two years as Council President. He is a past Editor of the IEEE JOURNAL OF SOLID-STATE CIRCUITS, a member of the Solid-State Circuits Society AdCom, and is now President of the Society. He was Program Chairman for the 1993 International Solid-State Circuits Conference, and Chairman of the 1990 VLSI Circuits Symposium. From 1980 to 1982 he served as founding Editor-in-Chief of IEEE MICRO, and subsequently received an Outstanding Contribution Award from the IEEE Computer Society for development of that magazine. He was selected as one of the IEEE Computer Society's "Golden Core" and received an IEEE Third Millennium Medal. Dr. Jaeger was elected Fellow of the IEEE in 1986 and was appointed to the Distinguished University Professorship by Auburn University in 1990. He received the Birdsong Merit Teaching Award from the College of Engineering in 1991. In 1993, he was chosen as the Outstanding EE Faculty Member by the undergraduate students. In 1995, he was selected as the Distinguished Graduate Faculty Lecturer. In his spare time, he is an avid amateur radio operator (K4IQJ), enjoying dx and contest operation. He is a member of Sigma Xi, Phi Kappa Phi, Tau Beta Pi, Sigma Tau, a Licensed Professional Engineer, and was first listed in *Who's Who in America* in 1990.